Energy Conversion and Management: X 22 (2024) 100546

Contents lists available at ScienceDirect

Energy Conversion and Management: X

journal homepage: www.sciencedirect.com/journal/energy-conversion-and-management-x

Solar heat for the decarbonization of chemical industry: dehydrogenation of ethylbenzene to styrene driven by a concentrating solar power plant with molten salts as heat transfer fluids

Claudia Prestigiacomo [a], Federica Proietto [a], Alberto Giaconia [b], Monica Genovesi [a], Najwa Hamdi [a], Onofrio Scialdone [a], Alessandro Galia [a,*]

[a] Dipartimento di Ingegneria, Sezione Chimica Ambientale Biomedica Idraulica e dei Materiali, Università degli Studi di Palermo, Viale delle Scienze, 90128 Palermo, Italy

[b] ENEA - Italian National Agency for New Technologies, Energy and Sustainable Economic Development, Via Anguillarese 301, Rome 00123, Italy

ARTICLE INFO

Keywords:
Decarbonization
Concentrating solar power plant
Molten salts
Styrene production
GHG emissions

ABSTRACT

The dehydrogenation of ethylbenzene to styrene was used as a model of an energy intensive endothermic process to assess the economic sustainability of the utilization of solar heat from a concentrating solar power (CSP) plant to decarbonize an industrial chemical processes.

To this purpose a process configuration compatible with the hybridization with a CSP plant using a binary mixture $NaNO_3/KNO_3$, 60/40 w/w as heat transfer fluid (HTF) was selected.

The adopted chemical reactor is a shell and tube bundle converter with 30000 tubes of 6 m length and 0.025 m inside diameter that approaches isothermal regime with a productivity of 103 kT/year of styrene if a flowrate of 200 kg/s of molten salt at 560 °C are fed to the shell. The residual enthalpy of the HTF leaving the dehydrogenation reactor was further injected in the process by vaporizing and pre-heating ethylbenzene and dilution water.

A cash flow analysis of the hybridized plant was performed considering solar field of increasing size so that the required solar power of 45 MW can be supplied for longer period of the year. We found that a CSP plant of 70 collectors can decrease CO_2 emissions of about 50 % with a rate of return on investment (ROROI) of 9.1 % for the solar field of the hybridized plant and can grant 410 k€/year of economic benefit arising from the methane and the lower emissions of CO_2. This study demonstrates that solar heat can be used to decarbonize energy intensive endothermic chemical processes without economic penalty for the plant profitability.

Introduction

Industry covered about 37 % of the total energy consumption in 2015 and 2016 and chemical and petrochemical industries are among the largest energy consumers with an average annual growth of energy demand in the period 2000 – 2016 of 2 % associated with a 2.5 % yearly rate of increase in CO_2 emission [1].

Most of industrial chemistry productions are addressed to synthesis of macromolecular materials that are strategic in many applications.

In this context styrene (STY) is one of the most produced vinyl monomers with an annual turnover of $ 43 billion [2,3]. This large market is due to its versatility in end-uses as it can be polymerized and copolymerized easily to produce a wide variety of plastics, resins and elastomers such as polystyrene, styrene-acrylonitrile and acrylonitrile–butadiene–styrene copolymers [4].

Styrene can be produced by catalytic dehydrogenation of ethylbenzene (EB) at temperatures between 600 and 800 °C in the presence of dilution steam at total pressure close to ambient value. In most cases the operating conditions in commercial reactors are 620 °C and pressure close to the atmospheric value.

The reaction is highly endothermic and is carried out industrially in

Abbreviations: ANI, aperture normal irradiance; CAPEX, capital expenditure; COM, cost of manufacturing; DDB, double declining balance depreciation method; d_k^{DBB}, depreciation at the year k; DNI, direct normal irradiation; DCFROR, discounted cash flow rate of return; EB, ethylbenzene; GHG, greenhouse gas; IRR, internal rate of return (short name for DCFROR); OPEX, operating expense; ROROI, rate of return on investment; SCA, solar collector assemblies; STY, styrene.

* Corresponding author.
E-mail address: alessandro.galia@unipa.it (A. Galia).

https://doi.org/10.1016/j.ecmx.2024.100546
Received 7 November 2023; Received in revised form 3 February 2024; Accepted 5 February 2024
Available online 8 February 2024

Nomenclature

α	reciprocal of the adsorption coefficient of ethylbenzene
ΔH_r	reaction enthalpy (kJ mol^{-1})
ε	porosity of the porous beds (void fraction)
μ_{mix}	viscosity of the mixture tube side (μP)
ρ_{mix}	density of the mixture tube side (kg m^{-3})
ρ_{ms}	density of the molten salts shell side (kg m^{-3})
ρ_p	density of the catalytic pellet (g mL^{-1})
Cp_i	specific heat of i-compound (kJ kg^{-1} K^{-1})
Cp_{mix}	specific heat of the mixture tube side (kJ kg^{-1} K^{-1})
d_p	diameter of the catalytic pellet (m)
d_{pe}	equivalent diameter of catalytic pellet (mm)
f	friction factor
F_i	molar flowrate of i-compound (kmol h^{-1})
h_v	tube-side heat transfer coefficient (W m^{-2} K^{-1})
h_{ms}	shell-side heat transfer coefficient (W m^{-2} K^{-1})
kf_{mix}	thermal conductivity of tube side mixture (W m^{-1} K^{-1})
kf_{ms}	thermal conductivity of molten salts (W m^{-1} K^{-1})
l_p	lenght of the catalyst pellet (m)
L_{tubes}	length of the tubes of the reactor (m)
m_{pellet}	mass of the catalyst pellet (g)
$\dot{M}_{CH_4}$	consume of methane per month (kg)
MW_{av}	average molecular weight of the tube side mixture
M_i	mass flow rate of the i-compound
Nu	Nusselt number
P	total pressure (atm)
Pi	partial pressure of i-compound (atm)
Pr	Prandtl number
Q_m	thermal load in each month of the year (MJ)
r_i	reaction rate (kmol h^{-1} m^{-3})
Re_p	tube-side Reynolds number (tubes filled by cylindrical catalyst pellets)
Re_{ms}	shell-side Reynolds number
Ti_{tubes}	inlet tube-side temperature (°C)
Ti_{shell}	inlet shell-side temperature (°C)
To_{tubes}	outlet tube-side temperature (°C)
To_{shell}	outlet shell-side temperature (°C)
U	global heat exchange coefficient (kJ m^{-2} h^{-1} $°C^{-1}$)
v	spacial velocity (m/s)
V_p	catalyst pellet volume (m^3)
V_{pores}	pores volume of the catalyst (mL)
X	conversion
W/F	contact time (W mass of catalyst, F moles of ethylbenzene/h)
z	relative adsorption coefficient of styrene on the catalyst

both adiabatic and isothermal reactors [5]:

$$C_6H_5CH_2CH_3 \leftrightarrow C_6H_5CH = CH_2 + H_2 \ \Delta H_r(600\ ℃) = 124.9\ kJ/mol \quad (1)$$

Competing reactions degrade ethylbenzene to benzene and to coke and hydrogen:

$$C_6H_5CH_2CH_3 \leftrightarrow C_6H_6 + C_2H_4 \ \Delta H_r = 101.8\ kJ/mol \quad (2)$$

$$C_6H_5CH_2CH_3 \leftrightarrow 8C + 5H_2 \ \Delta H_r = 1.72\ kJ/mol \quad (3)$$

The catalytic system also allows, albeit with modest yields, demethanation to toluene:

$$C_6H_5CH_2CH_3 + H_2 \leftrightarrow C_6H_5CH_3 + CH_4 \ \Delta H_r = -64.5\ kJ/mol \quad (4)$$

At previously mentioned operative conditions (620 °C and 1 atm) the reversible reaction (7) results in an equilibrium conversion of ethylbenzene of about 80 % but the time required to reach equilibrium results in excessive thermal cracking and selectivity loss, so most commercial units operate under kinetic control with ethylbenzene conversion limited to 50–70 % per pass and selectivity to styrene greater than 90 % [6].

Many catalysts have been proposed to activate reaction (1) and among them the most used is Shell 105 that consists of 84.3 % Fe_2O_3, 2.4 % Cr_2O_3 and 13.3 % K_2CO_3 and was the first to include potassium as promoter of the iron oxide active phase [7].

This catalyst was selected as a reference in this study.

To carry out the process with good performances dilution of the gasified aromatics with steam is mandatory to lower the partial pressure of hydrocarbons thus minimizing the rate of thermal cracking reactions.

Steam plays also the role of enthalpy vector to drive the endothermic cleavage and decreases the net rate of catalyst fouling as, in the presence of the potassium promoters, gasify the deposited carbon by conversion to carbon dioxide and hydrogen.

The choice of the process as model case study for the decarbonization of industrial chemistry is also motivated by the marked interest in finding sustainable alternative production methods because of its high energy requirements and reliance on fossil fuels.

Use of solar heat for the decarbonization of chemical processes was initially investigated studying the conversion of natural gas, oil and coal to hydrogen and carbon/carbon dioxide that can be addressed to sequestration [8,9]. The research activity extended to solar heat driven conversion of carbonaceous feedstocks, including biomass, in hydrogen and syngas by thermochemical processes such as cracking/pyrolysis, reforming/gasification, and two-step chemical looping processes using metal oxides as oxygen carriers as recently thoroughly reviewed [10–15]. Other decarbonization strategies involving chemical processes are based on the capture of CO_2 and its conversion to methanol assisted by solar heat [16].

Different technologies have been conceived and developed so far to concentrate the incoming direct solar irradiation (DNI) on a solar receiver element to generate high-temperature heat (at T > 350 °C). These include point and linear focusing systems, depending on the geometry of solar collectors and receivers, resulting on different concentration rates [17]. Each technology has specific features making it more suitable in specific scenarios, depending of the plant location and size, land availability, environmental constraints, etc. Current solar tower plants with central receivers allow to produce heat at temperatures up to 550–600 °C or more and, therefore, are suitable for high efficiency power generation. Linear focusing systems, such as troughs and Fresnel collectors, are modular technologies that commonly use thermal oils as heat transfer fluid up to 400 °C; innovative linear focusing plants use molten salts to produce heat to temperatures higher than 500 °C equipped with thermal energy storage (TES) systems to generate dispatchable power [18]. Recent studies show the trend to investigate advanced salts with improved heat transfer properties and stable at higher temperatures in order to increase the storage capacity and the overall efficiency of the thermal cycle [19].

In this study we investigated the possibility of increasing the sustainability of an already existing industrial chemical process such as styrene production by using solar heat stored in molten salts as heat transfer fluids in substitution of methane combustion. By the adoption of TES in fluid media, such as molten salts, the solar heat can be used in conventional chemical reactors that are a more simple technological option with respect to directly irradiated cavity [20–24], or volumetric receiver [25–27] solar reactors. Anyway the practical implementation of this integration is complex and not obvious because requires the development of a strategy to match economically the intermittent nature of sun radiation with the continuous operation of a chemical plant

addressed to the production of a commodity product. Indeed, in the aforementioned context, the dehydrogenation of ethylbenzene to styrene can be taken as a model of endothermic processes with a high energy demand and heavy carbon footprint and the results of the study of its decarbonization using solar heat can be adapted to other similar chemical industry productions.

The scientific contribution of our study is the definition of a process lay-out and the formulation of a generally applicable strategy to integrate high temperature solar heat collected by a CSP plant, based on current state of the art technology, in a conventional catalytic fixed bed chemical reactor operated at steady state conditions.

The first part of the research activities concerned the study and selection of functional interfaces to couple the two technologies performing the chemical route with performances compatible with industrial production. Then we studied the economic sustainability of this strategy taking into account as source of revenue the saved cost of unburned fuel and not emitted CO_2.

Proposed chemical plant scheme

From a literature review we found a process technology developed by BASF (Fig. 1) to perform the dehydrogenation of ethylbenzene using a fixed bed bundle isothermal reactor. In this plant, most of the enthalpy of reaction is provided by a furnace (element a in Fig. 1) that heats a molten salt mixture at about 630 °C. Hot molten salts are fed to the shell of the catalytic reactor with the catalyst located inside tubes (element c in Fig. 1) in which a gaseous mixture of steam and ethylbenzene, at weight ratio of 0.6 to 0.9, is fed at near atmospheric pressure. Further enthalpy of the molten salt is used to generate dilution steam in heat exchangers (element d in Fig. 1) while a second furnace (element b in Fig. 1) is used to superheat the steam up to 600 °C [28].

The conceptual design of the integrated CSP-chemical plant was based on the aforementioned process configuration with the only modification that the two fuel furnaces a and b are substituted by the CSP plant [6].

Then the economic sustainability of the integration was evaluated at fixed plant productivity comparing the costs of the CSP plant with the money saved for the lower amounts of emitted CO_2 and consumed methane. From the study, it was found that the size of industrial plants for the production of styrene from ethylbenzene using isothermal reactors averages around 100000 tons of styrene produced per year with a conversion of ethylbenzene close to 65 %. Based on this observation, a flow rate of ethylbenzene of 180 kmol/h was fixed and treated with a steam to ethylbenzene weight ratio of 3 at operating pressure of 1 atm. Inlet temperatures of molten salts in the reactor shell cannot be higher than 565 °C that is the maximum value achievable in the receivers of the CSP plant without degrading their coatings.

The HTF leaving the solar field at its maximum temperature (T_{max}) will transfer sensible heat to the process with the rate $(\dot{Q})$ linked to its flow rate $(\dot{M}_f)$ and its temperature drop $(T_{max} - T_{min})$ according to the following equation (5):

$$\dot{Q} = \dot{M}_f \times C_{p,f} \times (T_{max} - T_{min}) \tag{5}$$

where $C_{p,f}$ is the specific heat of the HTF. Therefore, the approaching of an isothermal regime for the dehydrogenation reactor operating at a temperature much lower than T_{min} can be obtained only using a large flow rate $(\dot{M}_f)$ of the heat transfer fluid with a consequent small temperature drop $(T_{max} - T_{min})$ in the shell of the reactor. This means that the temperature of the molten salts exiting from the dehydrogenation reactor (T_{min}) is still too high to re-enter in the solar field as coolant of the collectors (usually, the temperature increase of the HTF in the solar field is > 100 °C). This constraint about the thermal coupling between an isothermal reactor operating at relatively high temperatures and a concentrating solar plant was already considered in previous studies, such as in solar steam reforming [29,30] and a steam generation unit was included to recover further part of the residual enthalpy of the HTF thus significantly lowering its temperature before the recirculation to the solar field. In the case study analyzed in this paper, the large residual enthalpy was used to generate and superheat the dilution steam thus avoiding the need of furnace b in Fig. 1.

Concentrating solar power plant layout

The layout of the concentrating solar plant was based on a proprietary technology developed by ENEA and already used to collect solar heat for the cogeneration of electricity and heat [18].

The design of the plant was carried out using as a first input

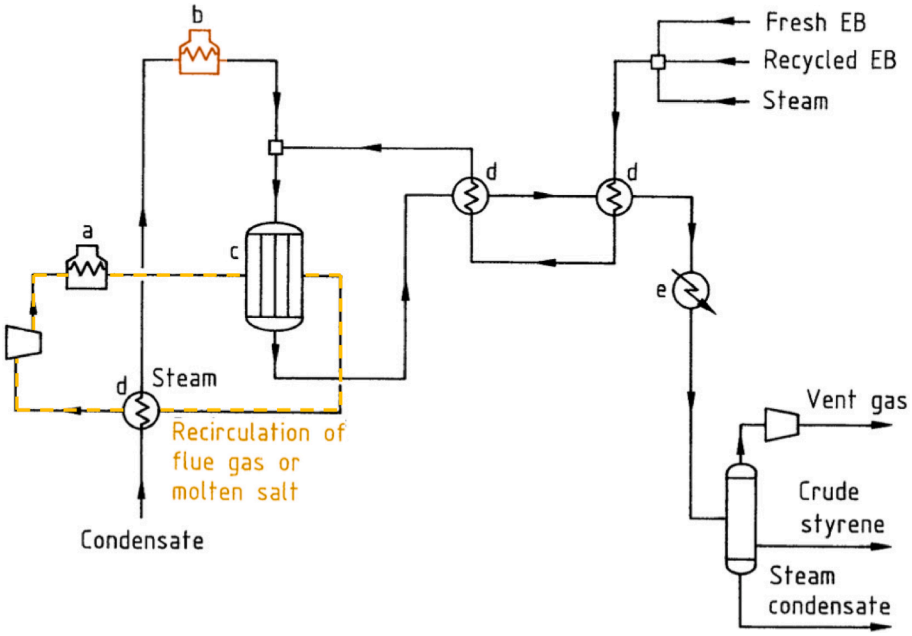

Fig. 1. Process diagram of the BASF plant for isothermal dehydrogenation of ethylbenzene adapted from [6] a)heater; b)steam superheater; c)bundle reactor; d) heat exchanger; e) condenser.

parameter the direct normal irradiance (DNI).

In this study, the DNI sequence in the site of Priolo Gargallo in Sicily (Italy) (37° 9.18′ N; 15° 10.56′ E) recorded during the years 2006–2012 with average DNI value of 221 W/m^2 has been assumed as a reference [31].

To size the CSP plant, its coupling with the chemical process and the fraction of incident solar radiation actually collected by the surface of the receiver tubes, namely the aperture normal irradiance (ANI), were determined for each DNI sequence. The ANI is lower than the DNI because it includes only the mirror-normal solar radiation component, proportional to the cosine of the angle between the direction of sun's rays and the normal direction to the collector. The ANI also considers shading effect between solar collectors that depends on the distance between their rows.

The ANI distribution was calculated from DNI using the eq. (6):

$$ANI = DNI \times K_{mod} \times R_{ow}S_{hadow} \times E_{nd}L_{oss} \quad (6)$$

where K_{mod} is the incidence angle modifier that is given by an empirical equation obtained from the fitting of experimental data for a given type of collector, $R_{ow}S_{hadow}$ provides the shadowing effect and $E_{nd}L_{oss}$ the end loss effects due to incomplete reflection of the incoming sun rays on the solar receiver in the ends of linear solar collector rows.

In the case of collectors typically adopted by ENEA and considered in this study the fitting equation to determine K_{mod} is reported in eq. (7):

$$K_{mod} = \cos\vartheta + 9.511E-4 \times \vartheta - 3.218E-5 \times \vartheta^2 \quad (7)$$

where ϑ is the incidence angle of solar radiation, i.e. the angle formed by the direction of the beam radiation on a surface and the normal direction to that surface. The incidence angle will vary over the course of the day, as well as throughout the year, and will heavily influence the scavenging performance of the collectors. $R_{ow}S_{hadow}$ and $E_{nd}L_{oss}$ in eq. (6) can be determined by eq. (8) and (9):

$$R_{ow}S_{hadow} = \left(L_{spacing}/W\right) \times (\cos\vartheta_z/\cos\vartheta) \quad (8)$$

where $L_{spacing}$ is the center distance of two parabolic trough concentrators, W is the aperture width (5.8 m) and ϑ_z is the solar zenith angle.

$$E_{nd}L_{oss} = 1 - (L_f \times \tan\vartheta/L_p) \quad (9)$$

where L_f is the focal length and L_P is the length of parabolic trough (having values of 1.81 and 100 m respectively in the solar field under consideration).

The as-determined typical ANI sequences in Priolo is reported in a previous study [16]. Calculation were conducted with the linear parabolic collector (solar trough) technology considered by ENEA in previous studies [18,29,31].

In Priolo an average value of the ANI specific collected solar power of 178 W/m^2 was found with a maximum radiation value of 964 W/m^2 and an annual integral value of 1556 kWh/(m^2 y).

The monthly distribution of the daily mean value of ANI in Priolo is plotted in Fig. 2.

Concentrating solar power plant design and layout

The CSP plant considered in this study is based on linear parabolic trough collectors made of 100 m long solar collector assemblies (SCA) with 5.8 m effective mirrors' width, according to a design demonstrated by ENEA in previous projects [18].

A binary mixture $NaNO_3/KNO_3$, 60/40 w/w, namely the "solar salt", has been considered as heat transfer fluid (HTF) up to 565 °C [32].

The CSP plant consists of several loops (from 50 to 100 as explained in the following sections) composed of six SCAs, each 100 m long (Fig. 3). Therefore, in total, the HTF must flow in each loop for 600 m of linear pathway in the receiver tubes to collect the concentrated solar radiation.

The molten salt is pumped from the cold tank (around 423 °C) through the parallel loops of the solar field where it is heated up to 565 °C and, then, collected in the hot storage tank. For a given value of the DNI (and ANI), the flow rate of the HTF is tuned to be heated at the target temperature of 565 °C in each loop of the solar field according to the strategy that the lower the ANI, the lower the molten salt flow rate. The flow rate of molten salts q in each loop can reach a minimum value of 1.5 kg/s: therefore, when the ANI falls below a threshold value (e.g. after sunset or during cloudy periods) the HTF is recirculated in each loop of the solar field at its minimum rate of 1.5 kg/s and, if the outlet temperature of 565 °C could not be reached, the outlet molten salt (at T < 565 °C) is directly recirculated to the cold tank because its enthalpy will not be high enough for the cleavage of ethylbenzene. In this situation, if the temperature of the HTF exiting the solar field will be higher

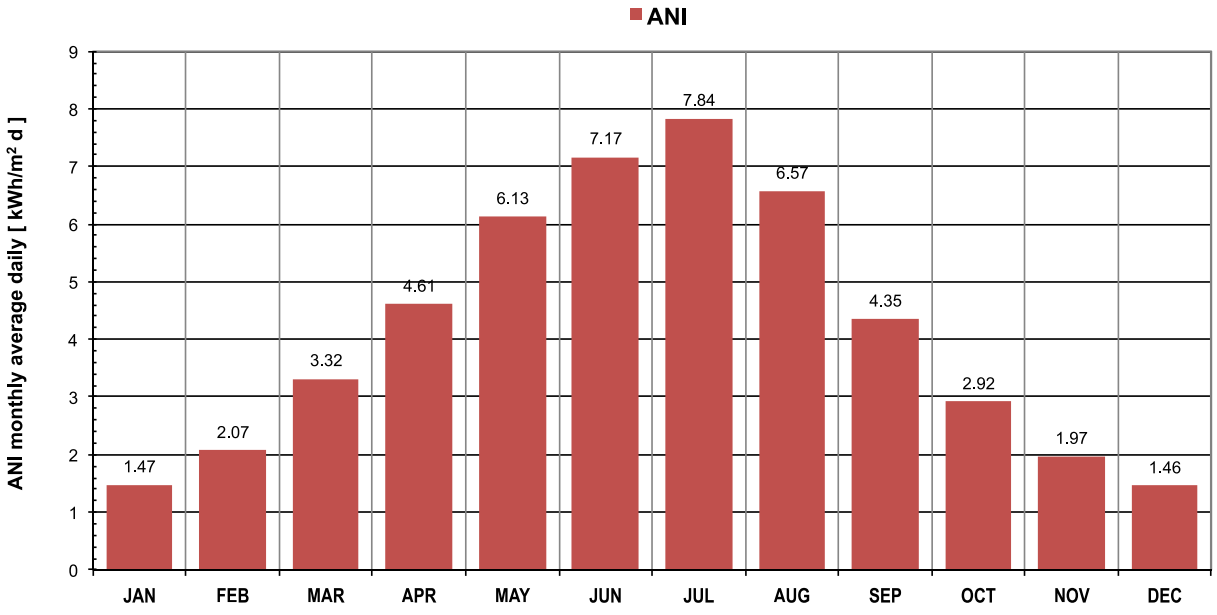

Fig. 2. Monthly distribution of the daily mean value of ANI for Priolo.

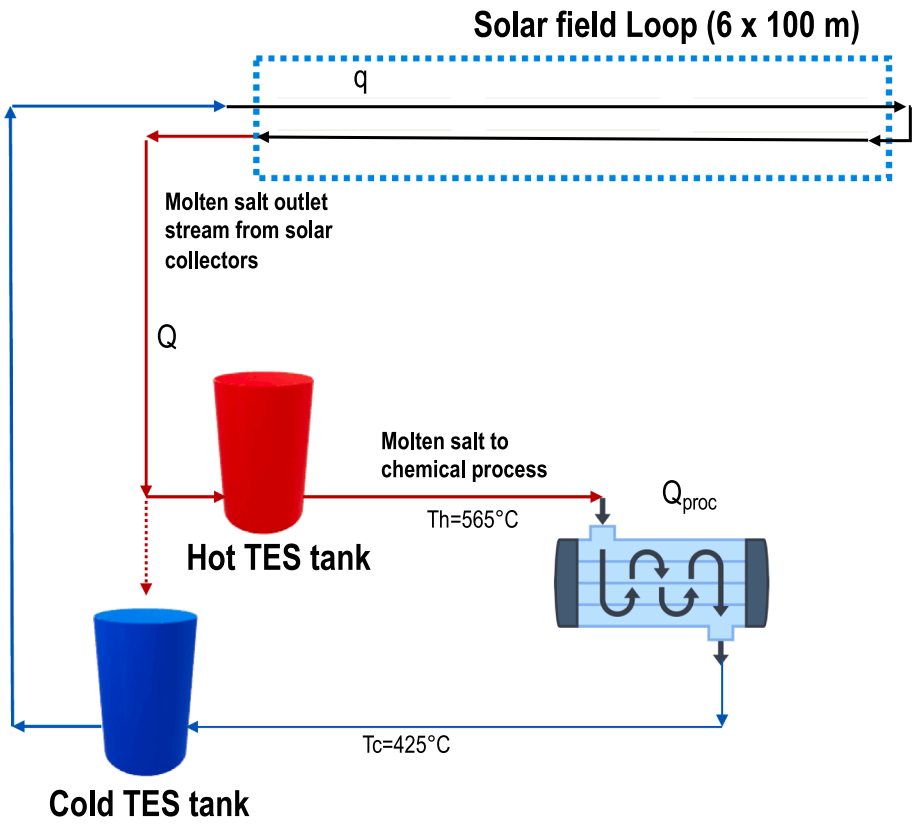

Fig. 3. Scheme of one solar collectors loop (consisting of 6x100 m linear collectors) composing the modular solar field and block diagram of the molten salt loop to the heat load. q is the flow rate of HTF in each loop (minimum value 1.5 kg/s), Q is the total HTF flow rate collected from the hot TES, Q_{proc} is the HTF flowrate sent to the chemical process.

than 423 °C (but still lower than 565 °C) the recirculation will increase to some extent the temperature of the salt stored in the cold tank; therefore, this heat could not be directly used to drive the chemical process but, being stored in the cold tank, it can be recovered to compensate heat losses during the night circulation of the HTF in the solar field [18].

It must be underlined that the flow rate sent to the hot TES tank is given by the product nq, where n is the number of loops, and that the flow rate pumped from the hot TES to the chemical reactor can be also higher than this value thanks to the storage capacity of the vessel.

The efficiency of the solar field is given by the ratio between thermal energy effectively transferred to the HTF and the normal irradiance on collectors, i.e. the ANI (W/m^2) multiplied by the effective reflecting area of collectors; typical factors affecting the efficiency of the solar field have been considered, including solar tracking errors, geometric factors, reflectance of clean mirrors, receiver tubes absorbance, dust effects on mirrors reflectance and receiver tubes absorbance, etc.

The operation of a modular design of this kind of solar field has been recently demonstrated by ENEA [18].

The daily captured solar heat and the number of hours the chemical process can be driven by solar heat increases with the number of 600 m length rows connected in parallel, provided that the TES has the capacity of storing all captured solar heat at 565 °C. This matching extend the solar operation of the chemical plant for a number of hours when the direct normal solar irradiation (DNI) drops.

Mathematical model of the chemical reactor

Some assumptions were made to perform the technical–economic evaluation of the hybridized plant:

- the adopted chemical reactor is an isothermal shell and tube fixed bed reactor;
- plug-flow was assumed in the catalyst-filled tubes and in the shell of the reactor;
- hot molten salts and cold reaction mixture were placed in pure equicurrent;
- determination of the heat transfer coefficients inside the tubes and in the shell was carried out using dimensionless correlations reported in the literature [33];
- along the entire length of the catalytic bed, changes in temperature, conversion and pressure were estimated by integrating the energy, mass and momentum balance equations assuming the absence of radial gradients;
- the reactor length was determined by fixing to 0.7 atm the maximum pressure drop in the tubes;

the highest allowable reaction temperature was fixed by the maximum temperature of the molten salts entering in the shell side of the reactor (from 550 to 565 °C).

At these temperatures the ethylbenzene dehydrogenation reaction was considered the only one operating in the reactor, as indicated by the experimental studies conducted by Carrà and Forni [34] that found an almost quantitative selectivity to styrene at temperatures close to 550 °C in the presence of Shell 105 catalyst.

The reaction rate was modeled by equation (10) [34] that matches quite well the kinetics of the process in the temperature range from 495 °C to 630 °C:

$$dX/d(W/F) = \frac{k_1(P_E - P_H P_S/K)}{\alpha + P_E + zP_S} \quad (10)$$

where X is the EB conversion; W/F is the contact time (W: g of catalyst, F:

moles of ethylbenzene/h); P_E, P_H and P_S are the partial pressures of ethylbenzene, hydrogen and styrene, respectively; k_1 is the kinetic constant; z is the relative adsorption coefficient of styrene expressed as ratio between the adsorption coefficient of the vinyl compound and that of ethylbenzene; α is the reciprocal of the adsorption coefficient of ethylbenzene; and K is the equilibrium constant of eq. (1) given by eq. (11) as a function of temperature:

$$lnK = -15350/T + 16.12 \tag{11}$$

Conversion, temperature and pressure profiles in the tubes and in the shell were estimated by simultaneous solution of the differential equations of the energy, mass and momentum balances using Euler's method. All calculations were performed using Microsoft Excel ® software.

The properties of Shell 105 catalyst are listed in Table 1.

The void fraction ε, used in the Ergun equation, was estimated by the correlation reported in Banyahia et al. [35].

$$\varepsilon = a + \frac{b}{\left(d_t/d_{pe} + c\right)^2} \tag{12}$$

where d_t is the tube diameter, d_{pe} is the equivalent diameter of the pellet and a, b and c are dimensionless parameters that in the case of the selected Shell 105 cylindrical pellets have the values $a = 0.373$, $b = 1.703$, $c = 0.611$.

The chemical and physical properties of each single component of the reacting mixture (specific heat, viscosity, thermal conductivities, etc.) were taken from Perry, R. H., & Green, D. W. (2008) [36]. The mixture values were estimated using molar fraction based averages.

The properties of the molten salt mixture were estimated by referring to an earlier study by ENEA, reported in [37].

The energy (tube-side and shell-side), mass and momentum balances can be written in finite difference mode. All values and correlations adopted in this study are listed in Table 2.

Table 1
Properties of the Shell 105 cylindrical catalyst used in this study.

Properties	Value	Unit
Density of the pellet (ρ_p)	2.68	g/mL
Diameter of the pellet (d_p)	0.003	m
Lenght of the pellet (l_p)	0.003	m
Volume of the pellet (V_p)	2.10E-08	m^3
Pores volume (V_{pores})	0.0102	mL
Mass of the pellet (m_p)	0.0568	g
Aspect ratio (l_p/d_p)	1	
Equivalent diameter of the pellet (d_{pe})	2.6	mm
Void fraction (ε)	0.38	

Methodology for the economic assessment

In order to assess the economic sustainability of the proposed strategy, a market survey was carried out to estimate the costs of methane and the related social cost of carbon (SCC) i.e. the cost that the industrial site must pay annually for the quantities of CO_2 emitted in the atmosphere.

It has been seen that at the end of 2021, the average cost of methane was about 1169.00 € / ton while the SCC was around 96.00 €/ ton [38] and these values were set as reference.

The tons of CO_2 emitted by the unit without coupling with the solar system and those emitted considering the integrated solar system were estimated. It has to be considered that, even if in the integrated system the traditional furnace was substituted with CSP, during the year, some back up energy has to be provided to the plant to compensate the seasonal reduction of solar radiation. In some days of the year, especially in winter, the sun radiations are not enough to heat the molten salt mixture till the reaction temperature, and for this reason the hot reservoir of molten salts goes to its exhaustion. An additional boiler (back-up oven) is usually joined to the solar plant to heat the mixture to the reaction temperature when the direct solar irradiation is not enough to reach the desired target temperature of 565 °C. Specific molten salt heaters (MSH) have been developed, designed and demonstrated to the pilot or pre-commercial scale to serve as back-up units for CSP plants [18,39].

The calculation of the tons of CO_2 emitted by the furnace of the BASF plant and by back-up oven was made following the Tier 1 approach reported in IPCC guidelines of 2006 [40], which refers to the consumed fuel during stationary combustion processes. Following the methodology of Tier 1, we used the fuel consumption ($E^{Fuel_j}_{(column_i)}$) and emission factor $\varepsilon^{Fuel_j}_{CO_2}$ as reported in eq. (13) to determine the amount of emitted CO_2:

$$M^{Fuel_j}_{CO_2} = E^{Fuelj} \times \varepsilon^{Fuel_j}_{CO_2} \tag{13}$$

where $M^{Fuel_j}_{CO_2}$ represents the mass (kg) of carbon dioxide emitted for each kind of consumed j type of fuel (kg of greenhouse gases GHG), $E^{Fuelj}_{(i)}$ is the j fuel consumption expressed in TJ i.e. the mean the energy developed

Table 2
Correlation adopted in the modeling of the reactor.

	Correlation description	equation
1	energy balance tube side	$\Delta T_{tubes}/\Delta z = \frac{USN_t\left(T_{shell}\vert_z - T_{tubes}\vert_z\right) + dX/d(W/F)F^0_{ethylbenzene}S\rho_P\Delta H^0_r}{Cp_{mix}\sum M_i}$
2	energy balance shell side:	$\Delta T_{shell}/\Delta z = \frac{USN_t\left(T_{shell}\vert_z - T_{tubes}\vert_z\right)}{Cp_{ms}M_{ms}}$
3	mass balance of the ethylbenzene:	$\Delta F_{ethylbenzene}/\Delta z = dX/d(W/F)F^0_{ethylbenzene}S\rho_P$
4	momentum balance was implemented using the steady-state momentum equation from Ergun	$\Delta P/\Delta z = \frac{150\mu}{d_p^2}\frac{(1-\varepsilon)^2}{\varepsilon^3}v + \frac{1.75\rho(1-\varepsilon)}{d_p\varepsilon^3}v^2$

Where: Δz is the thickness of the cylindrical elemental volume selected for the calculations; ΔT_{tubes} represents the tube side change of temperature of the reaction mixture between z ($T_{tubes}\vert_z$) and z + Δz ($T_{tube}\vert_{z+\Delta z}$); U is the local global heat exchange coefficient; S is the cross-sectional area of passage of the fluid inside the tubes; N_t is the number of tubes of the reactor; $T_{shell}\vert_z$ is the temperature of the mixture of molten salts in the shell at z; $T_{tubes}\vert_z$ n is the temperature of the reaction mixture in the tubes at z; $dX/d(W/F)$ is the incremental elemental EB conversion obtained by eq. (10);$F^0_{ethylbenzene}$ is the initial molar flow rate of ethylbenzene entering in the tubes; ΔH^0_r is the enthalpy of reaction at $T_{tubes}\vert_z$; Cp_{mix} is the specific heat of the reaction mixture calculated at $T_{tubes}\vert_z$; M_i are the mass flow rates of the components of the reaction mixture; ΔT_{shell} is the temperature change of molten salts in the shell between z and z + Δz; Cp_{ms} is the specific heat of molten salts at $T_{shell}\vert_z$; M_{ms} is the mass flow rates of molten salt mixture;$\Delta F_{ethylbenzene}$ is the difference in the molar flow rate of ethylbenzene calculated between z + Δz and z; ΔP is the pressure drop in the catalyst loaded tube calculated between z + Δz and z; is the reaction mixture viscosity calculated at z; v is the local space velocity of the reaction mixture in the tube at z.

by the burned fuel and $\varepsilon_{CO_2}^{Fuel_j}$ is the emission factor of the j fuel (kg GHG/TJ).

The emission factors of natural gas was taken by the IPCC guidelines of 2006, i.e. 56100 kg/TJ.

Table 3
Operating parameters adopted in the reactor design.

Design Parameters	Values
ID tubes [m]	0.025
flow rate of molten salts to the chemical process[kgs^{-1}]	200
F_{EB} [$kmolh^{-1}$]	179.2
F_{steam} [$kmolh^{-1}$]	3171.0
$T_{i(tubes)}$ [°C]	550
$T_{i(shell)}$ [°C]	565

The assessment of the coupling of the industrial process with concentrating solar plant was made following the Discounted Cash Flow method. The capital costs to determine the capital investment cost (CAPital EXpenditure - CAPEX) of the solar system were estimated by ENEA staff on the basis of internal skills and tools. More in detail, ENEA considered the effective costs sustained for the realization of a fully-equipped CSP demo plant (with Thermal Energy Storage, TES, MSH back-up unit and steam generator) to supply about 5 MW heat rate to a co-generation (heat and power) process [18]. The units of the CSP plant (including heat exchanges, TES, etc.) have been scaled-up and costs estimated using the typical engineering practices for rough estimate of the CAPEX. This methodology has been validated by ENEA after exchange with CSP plant developers.

The investment costs related to heat exchangers and furnaces were calculated using the cost indices from Turton et al. [41]. The OPEX, i.e. operating expenditure or cost of manufacturing (COM), of the CSP plant

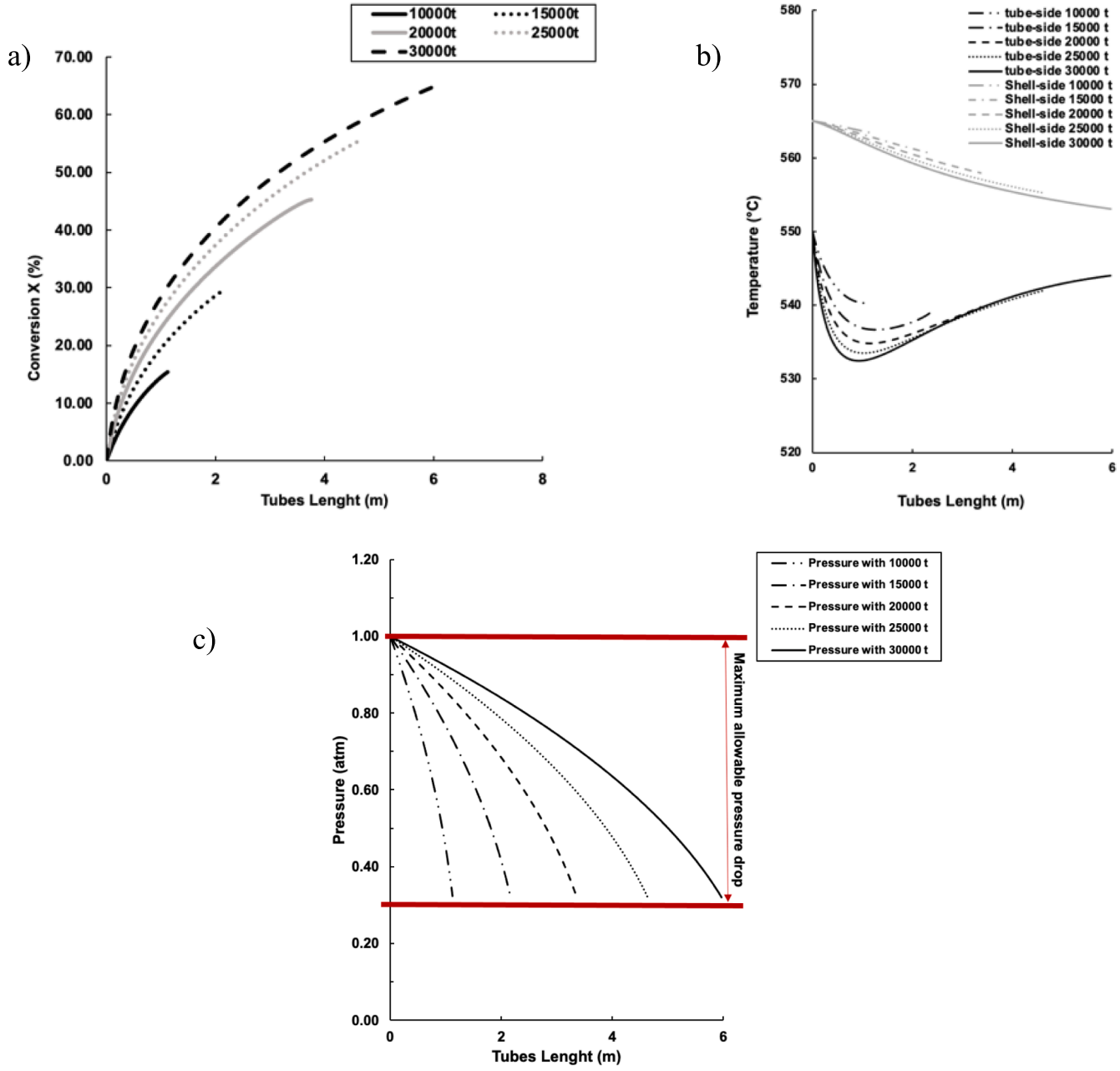

Fig. 4. A) Conversion profiles, b) temperature profiles and c) pressure drop for shell and tubes reactors designed varying the numbers of tubes, with the nominal characteristics reported in Table 3 and the maximum allowable pressure drop fixed to 0.7 atm.

was estimated at 0.03 USD / kWh (i.e. 0.027 € / kWh) as reported in the IRENA report on the analysis of renewable energy costs [42].

The rate of return on investment (ROROI) which represents the undiscounted rate at which the money is obtained from the investment of fixed capital considered, was estimated as per eq. (14), following an analysis of the cash flow considering a plant life of 20 years, with production starting from the 2nd year being the first dedicated to the construction of the solar plant.

$$ROROI = Averaged\ annual\ net\ profit/CAPEX \tag{14}$$

where CAPEX are the capital expenditures of the plant. The calculations were made assuming an investment interest rate of 10 % and a revenue tax rate of 40 %. Depreciation costs were considered using the double declining balance depreciation method, DDB over a 20-year period, calculated with equation (15):

$$d_k^{DDB} = 2 \Big/ n \times \left[CAPEX - \sum\nolimits_{j=0}^{j=k-1} d_j \right] \tag{15}$$

Where d_k^{DDB} is the depreciation at year k, calculated with the DDB depreciation method and n represent the total number of years. The discounted cash flow rate of return (DCFROR). also termed internal rate of return (IRR), was then estimated as the interest rate at which the net present value for each scenario is equal to zero [41].

Results and discussion

Design of the dehydrogenation reactor

The first step of the study was the design of the molten salt heated chemical reactor with an iterative method considering the operating parameters listed in Table 3.

With these values we compared the EB conversion of several reactors with numbers of tubes ranging from 10000 to 30000 with step of 5000 fixing the maximum allowable pressure drop to 0.7 atm value similar to that reached in the conventional industrial plant.

As styrene is a commodity chemical, ethylbenzene conversion close to 65 % must be reached in conventional industrial plant to make economically sustainable the process [6]. From Fig. 4 results that this value can be approached in the reactor with 30000 tubes of 6 m length.

The effect of the flowrate of recirculated molten salt inside the shell of the reactor was further investigated in the 6 m long bundle reactor with 30000 tubes changing the value from 50 to 200 kg/s and results in terms of conversions and temperature profiles are reported in Fig. 5. One can observe that when a flow rate as high as 200 kg/s was adopted a temperature drop in the tube-side stream of only 10 °C was estimated and the reactor approaches isothermal regime.

Further analysis were conducted to study the effect of the internal diameter of the shell tubes on the conversion, temperature and pressure profiles of reactors with 20000 and 25000 tubes (Fig. 6). Quite interestingly in these reactors an increase of ID of the tubes from 0.025 to 0.035 m can be used to decrease the linear velocity as well as the pressure drop and to increase the reactor length up to reach a conversion similar to that obtained with the 30000 tubes reactor.

Even if a conversion of 60–63 % was reached with all reactors, that with 25000 tubes and ID of 0.035 m would correspond, according to eq. (16) [43], to a bundle diameter of 13.5 m, that is 22 % larger of that obtained with 30000 tubes of 0.025 m ID and then more expensive; hence this configuration was excluded from further analyses.

$$D_{bundle} = \exp\left(\frac{(\ln N_t - ln 0.319)}{(2.142 + \ln(2 \times ID))}\right) \tag{16}$$

As already discussed in a previous section, the HTF flow rate necessary to approach a isothermal behavior of the reactor is very high (200 kg/s in Table 2) and the molten salts leaving the reactor shell still store large enthalpy that can be used to pre-heat water and ethylbenzene streams.

Energy integration was achieved using the hot mixture exiting the reactor tubes to preheat fresh liquid ethylbenzene mixed with 20 % of the dilution water and the molten salt leaving the reactor shell to generate the remaining part of steam by vaporizing and heating 80 % of the process water. By this choice the temperature of HTF pumped to the cold TES decreased to 423 °C.

However, by implementing this strategy in the calculations we found that the inlet reactor temperature of the reactants is lower than 550 °C. To adjust this value we added before the reactor an additional molten salt exchanger where the mixed steam/EB feed is heated up to 550 °C using in the shell side the hot molten salts at 565 °C that are cooled to 560 °C in this unit operation. The definitive process architecture for solar hybridization is highlighted in Fig. 7 together with the temperature of the process streams in the different points of the process.

After this lay-out adjustment, a second iteration of the reactor design was done that showed that the maximum attainable conversion is about

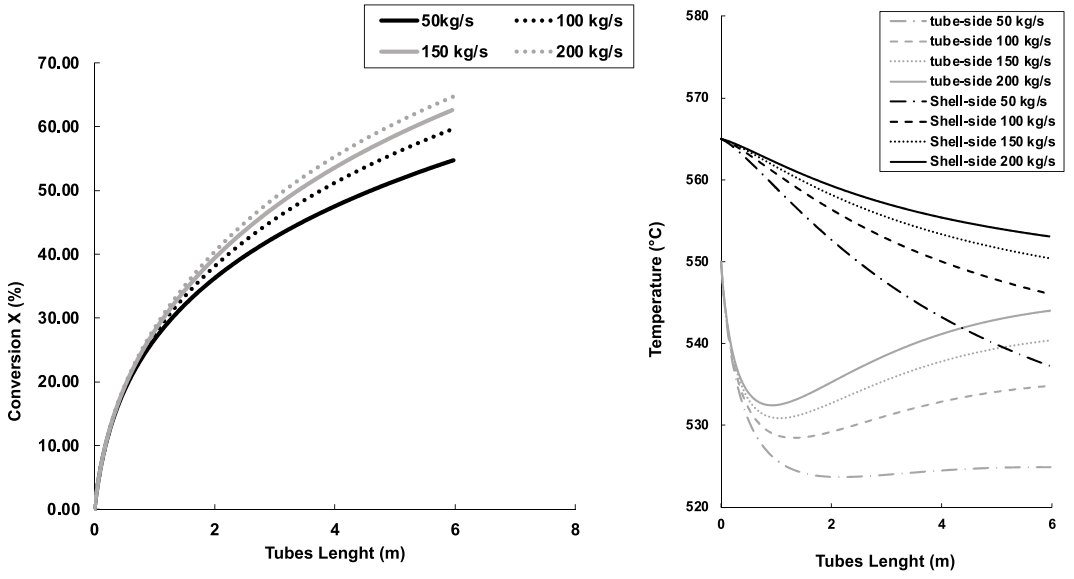

Fig. 5. Conversion (on the left) and temperature profiles (on the right) of the 6 m long reactor with 30000 tubes as a function of the flowrate of molten salts in the shell side.

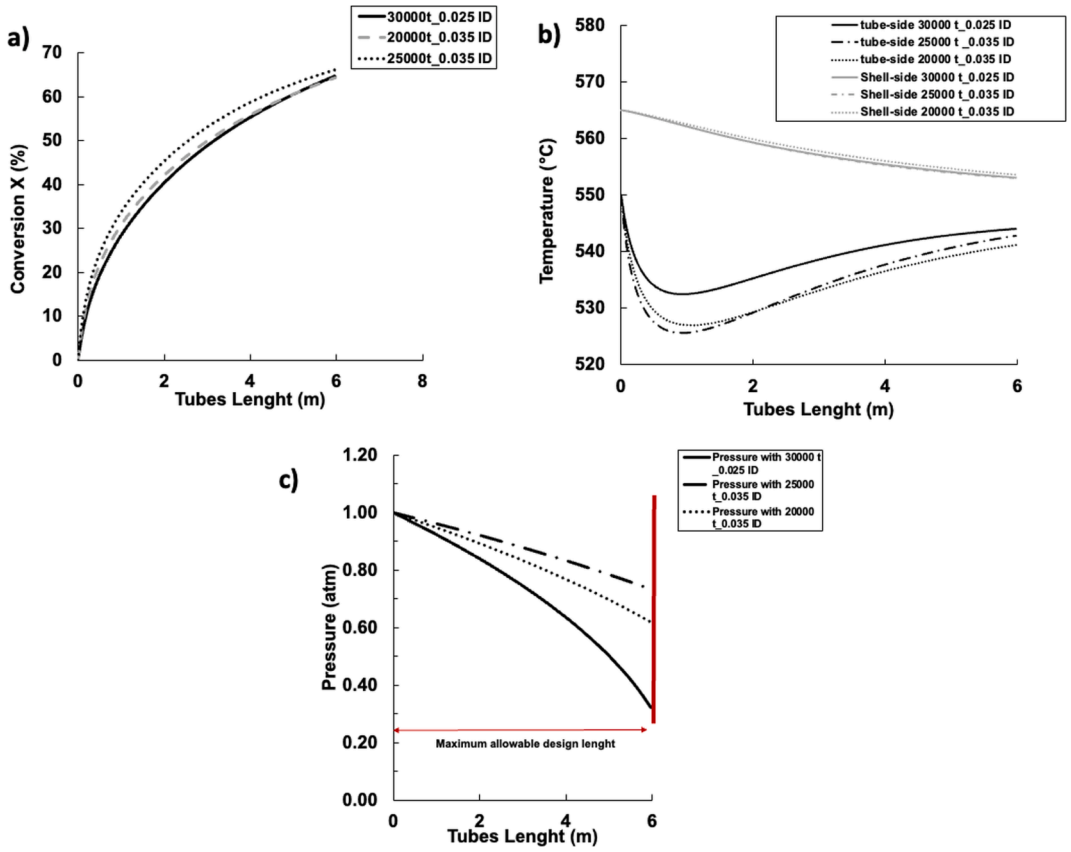

Fig. 6. A) conversion profiles, b) temperature profiles and c) pressure drop for shell and tubes reactors with 30000 tubes of 0.025 m ID and with 25000 and 20000 tubes with 0.035 m ID.

63 %, allowing a productivity of 103 kT/year of styrene similar to that achieved by the reference BASF plant developed at industrial scale. The data in Table 4 show that this result can be obtained with different volumes of the two reactors selected according to previous considerations. Reactor 2, characterized by a smaller volume and a smaller amount of catalyst inside the tubes, was chosen being more economical.

By aforementioned iterations we found a reactor geometry and size similar to that of a traditional fixed bed bundle reactor and we demonstrated that it can operate at quasi isothermal regime with a HTF flow rate that is compatible with a solar field equipped with 50–100 rows of parabolic through collectors. The significant residual enthalpy of the HTF leaving the isothermal reactor can be recovered by steam generation and ethylbenzene vaporization and pre-heating with a significant improvement of the decarbonization of the process.

Assessment of economic sustainability

To make a techno-economic assessment of the coupling of the ethylbenzene to styrene dehydrogenation process with CSP, the solar plant was sized considering a thermal flow rate transferred to the process fixed to 45 MW so that both the endothermic dehydrogenation and the steam vaporization stages could be simultaneously powered. The scenarios considered change by different areas of the solar plant (i.e., the number of considered loops of collectors). By this choice if the size of the solar field increases also the length of time in a year that the process can be driven by solar heat increases. This strategy allowed us to evaluate the effect of the numbers of solar loops on the reduction of CO_2 emissions for the decrease of operating time of the back-up furnace. Molten salts are stored in the hot TES at a temperature of 565 °C and sent to the cold TES at 423 °C, a temperature derived from the pre-heating of water that ensures efficient solar system sizing and minimizes the emptying time of the hot TES. To perform economic evaluations we used as a reference the BASF plant configuration that is already of industrial interest, and we estimated the costs of implementing the solar plant and heat exchangers in relation to the cost of non-consumed methane and not emitted carbon dioxide. In this framework the CAPEX and OPEX of the chemical plant and the selling price of the styrene are considered unchanged under the hypothesis that the economic sustainability of the hybridization with the solar plant is evaluated comparing the CAPEX and the OPEX of the CSP with the revenues from non-consumed methane and not emitted CO_2. The outcomes of the calculation of the economic analysis were used to define an annual normalized gain value (NGV), eq. (17), that constitutes the additional revenue that the chemical plant receive as a consequence of the hybridization with CSP.

$$NGV_{sty} = net\ profit\ value_{20}/20 \tag{17}$$

Where the *net profit value*$_{20}$ is calculated over 20 years.

To implement the hybridization the heat load of furnace a and b in Fig. 1 were replaced with the solar heat from the CSP considering the enthalpy absorbed by the endothermic cleavage and the heat required to vaporize and heat up to 550 °C liquid water at 25 °C. Then the fuel consumed for each individual month of the year ($\dot{M}_{CH_4}$) was determined according to eq. (18) considering an average lower heating value (LHV) of methane of 57 MJ/kg:

$$\dot{M}_{CH_4} = \dot{Q}m/LHV_{CH_4} \tag{18}$$

Where $\dot{Q}m$ represents the required heat per month (MJ).

Figs. 8 and 9 show the trends of CO_2 emissions as a function of the considered scenarios that are described in Table 5. When the number of solar collectors increases, the tons of CO_2 emitted decreases, especially in the summer months (Fig. 8).

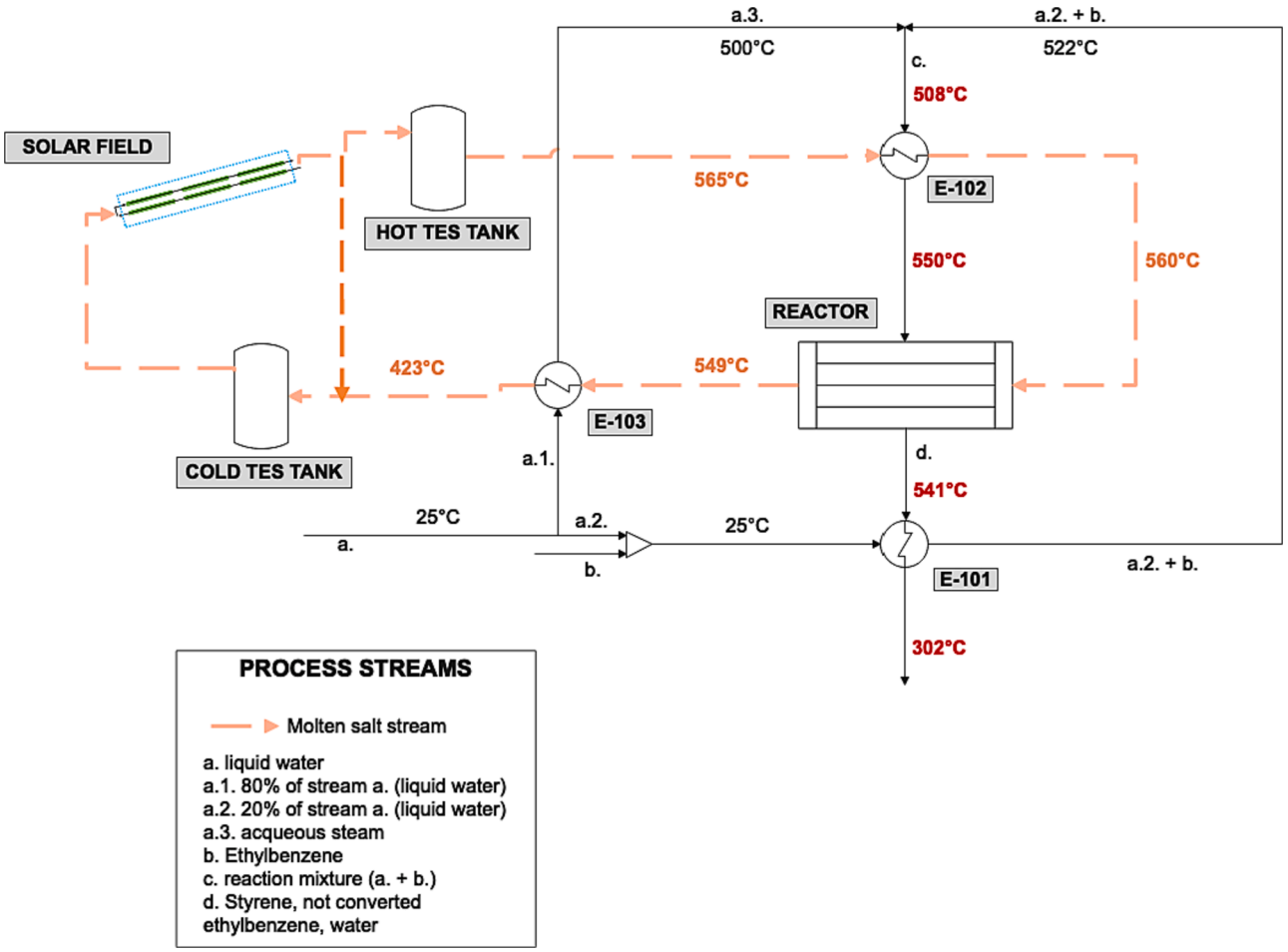

Fig. 7. Process diagram of ethylbenzene dehydrogenation plant coupled with a concentrating solar power plant.

Table 4
Optimized data for the final selection of the bundle reactor for the solar heat assisted dehydrogenation of ethylbenzene to styrene.

	Reactor 1		Reactor 2	
N_t	20000		30000	
ID tubes [m]	0.035		0.025	
$V_{reactor}$ [m^3]	462		353	
L_{tubes} [m]	6		6	
Catalyst [tonn]	773		590	
Molten salts [kgs^{-1}]	200		200	
X (conversion)	62.70		62.75	
	Inlet	Outlet	Inlet	Outlet
F_{EB} [$kmolh^{-1}$]	179.20	66.60	179.20	66.50
F_{ST} [$kmolh^{-1}$]	0.00	112.59	0.00	112.69
F_{H2} [$kmolh^{-1}$]	0.00	112.59	0.00	112.69
F_{TOT} [$kmolh^{-1}$]	3350.17	3462.76	3350.17	3462.86
M_{EB} [kgh^{-1}]	19025.88	7071.23	19025.88	7060.49
M_{ST} [kgh^{-1}]	0.00	11726.54	0.00	11737.06
M_{H2} [kgh^{-1}]	0.00	225.19	0.00	225.39
M_{water}[kgh^{-1}]	57077.63	57077.63	57077.63	57077.63
r_i [$kmolh^{-1}m^{-3}$]	2.52	0.081	2.52	0.12
K_{eq}	0.08	0.060	0.08	0.06
P_{EB} [atm]	0.05	0.012	0.05	0.01
P_{ST} [atm]	0.00	0.020	0.00	0.01
P_{H2} [atm]	0.00	0.020	0.00	0.01
T_{tubes} [°C]	550.00	537.79	550.00	540.62
T_{shell} [°C]	560.32	549.74	560.32	549.31
Cp_{EB} [kJ kg^{-1} K^{-1}]	2.70	2.68	2.70	2.68
Cp_{water} [kJ kg^{-1} K^{-1}]	2.17	2.16	2.17	2.16
Cp_{Sty} [kJ kg^{-1} K^{-1}]	2.53	2.51	2.53	2.51

Table 4 (*continued*)

	Reactor 1		Reactor 2	
Cp_{H2} [kJ kg^{-1} K^{-1}]	14.82	14.81	14.82	14.82
Cp_{ms} [kJ kg^{-1} $°C^{-1}$]	1.54	1.54	1.54	1.54
Cp_{Mix} [kJ kg^{-1} K^{-1}]	2.30	2.30	2.30	2.30
$\Delta H°r$ [$Jkmol^{-1}$]	123030.64	122953.16	123030.64	122971.28
kf_{mix} [$Wm^{-1}K^{-1}$]	0.07	0.07	0.07	0.07
μ_{mix} [μP]	269.59	266.81	269.59	267.79
$M_{Wav.}$	22.72	21.98	22.72	21.98
ρ_{mix} [kgm^{-3}]	0.34	0.201	0.34	0.11
u [ms^{-1}]	0.82	1.368	1.10	3.39
P[Kpa]	101.33	61.565	101.33	32.56
P[atm]	1.00	0.608	1.00	0.32
Re_p	26.49	26.763	34.60	34.84
Pr	0.86	0.881	0.90	0.88
Nu	9.46	9.579	10.80	10.88
hv [$Wm^{-2}K^{-1}$]	23.45	22.759	38.70	37.64
Re_{ms}	309.30	301.000	313.40	304.65
ρ_{ms}[kgm^{-3}]	1733.64	1740.364	1733.60	1740.64
kf_{ms}	0.55	0.547	0.50	0.55
H_{ms} [$Wm^{-2}K^{-1}$]	7.22	7.148	8.30	8.24
U [$kJm^{-2}h^{-1}°C^{-1}$]	19.87	19.582	24.70	24.33

It is considered, within the CAPEX of the solar plant, the cost of the heat exchangers designed to replace the BASF plant furnace b, the resulting CAPEX then used for the Discounted Cash Flow analysis. In detail, the capital cost was determined as a function of the heat transfer area, configuration and material. The heat exchangers E-101, E-102, E-103 in Fig. 7 were designed using stainless steel as manufacturing material. Table 6 reports more details of heat exchangers design.

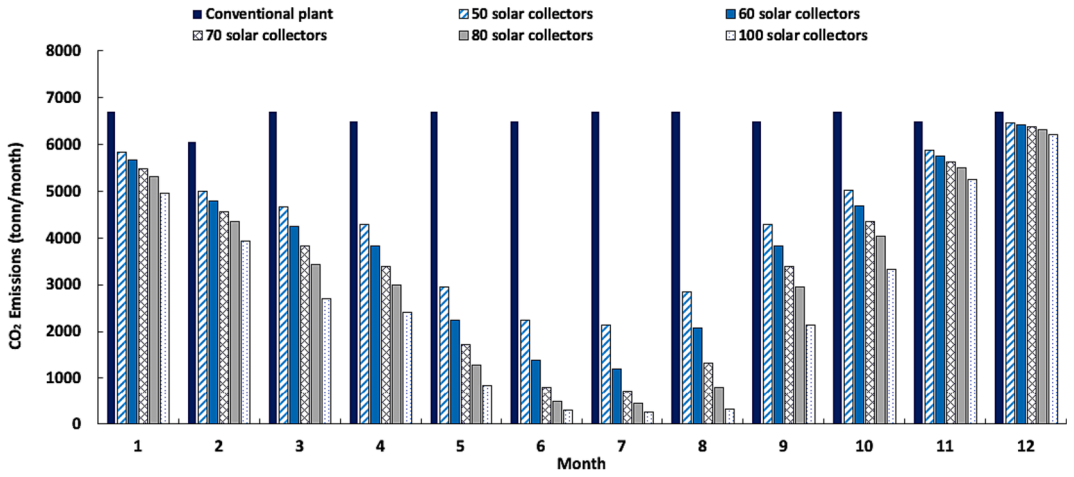

Fig. 8. Comparison of CO_2 emissions per month in the case of a plant totally driven by methane combustion (termed conventional plant), and of EB dehydrogenation plants hybridized with CSP plants according to the strategies of cases 1, 2, 3, 4 and 5 described in Table 5, i.e. changing the number of solar collectors from 50 to 100.

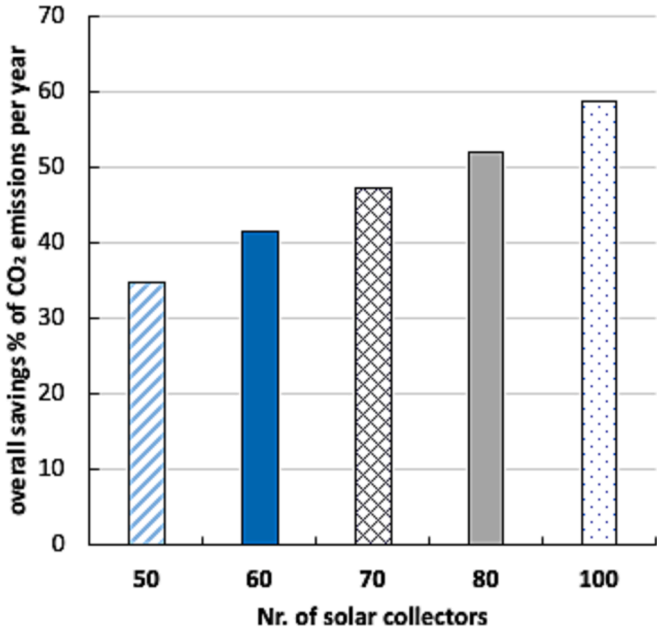

Fig. 9. Percentage of tons of CO_2 saved by coupling the ethylbenzene to styrene dehydrogenation process with the concentrating solar power plant (Cases 1–5 described in Table 5), i.e. changing the number of solar collectors from 50 to 100.

A salvage value of 10 M€ was considered for the CSP plant. Table 5 shows the CAPEX for the coupling cases assumed in the case of the ethylbenzene to styrene dehydrogenation process, and Fig. 10 shows the NGV, ROROI and DCFROR indices for each of the assumed scenarios. The latter, also termed internal rate of return (IRR), is currently adopted by economists and engineers to estimate the profitability (or potential profitability) of projects [44]. The capital cost of the replaced furnace and exchangers were estimated using the cost indices reported in [41] using CAPCOST tool.

Through the final evaluation of the discounted cash flow diagram (Fig. 11), of the rate of return on investment (ROROI) and of the discounted cash flow rate of return (DFCROR) carried out on these cases and plotted in Fig. 10, it can be concluded that for the cases 1, 2 and 3 ROROI and DFCROR fall within the range of 9.0 to 9.3 % and 10.9 to 11.9 % respectively. Additionally, it is important to take into account the trend of NGV value, i.e. additional revenue that the chemical plant receives as a consequence of the hybridization with the CSP plant. This value has a maximum when a solar field with 70 solar collectors is considered (case 3), but then decreases for larger solar field. This happens because, with larger CSP plant, part of the collected solar heat cannot be stored during some periods of the year. In these periods "dumping" conditions with solar power overproduction lead to wasting the excess incoming solar radiation (measured as dumping % in Table 5) by defocusing some collectors. Then the incremental cost of the CSP plant is accompanied by a lower incremental reduction of the emissions of carbon dioxide and for this reason is less economically compensated.

Table 5
Assessment of CAPEX due to coupling of reactor of dehydrogenation of ethylbenzene to styrene with CSP plant.

	Case 1	Case 2	Case 3	Case 4	Case 5
Nr. of solar collectors	50	60	70	80	100
Nominal Power to chemical plant (MW)	45	45	45	45	45
Area of the solar plant (m^2)	163,699	196,439	229,179	261,919	327,398
Cost due to the solar collectors and piping	35 M€	42 M€	50 M€	57 M€	71 M€
Cost of the pump	2 M€	2 M€	3 M€	3 M€	3 M€
Cost of the valves	1 M€	1 M€	1 M€	2 M€	2 M€
Cost of the salts	13 M€	13 M€	13 M€	13 M€	13 M€
Cost of the storage tank	1 M€	1 M€	1 M€	1 M€	1 M€
Other expenditures (insulation, electric parts, etc.)	0.3 M€	0.3 M€	0.3 M€	0.3 M€	0.3 M€
Furnace/boiler for back-up energy	1.7 M€	1.7 M€	1.7 M€	1.7 M€	1.7 M€
Cost of heat exchangers (E-101, E-102, E-103)	2.1 M€	2.1 M€	2.1 M€	2.1 M€	2.1 M€
Cost of the civil works due to the solar plant	3 M€	4 M€	4 M€	5 M€	6 M€
Conventional furnace (BASF plant) substituted by CSP	− 4 M€	− 4 M€	− 4 M€	− 4 M€	− 4 M€
CAPEX	55 M€	63 M€	72 M€	81 M€	96 M€
OPEX	4 M€	4 M€	5 M€	6 M€	6 M€
Savings of CO_2 (tonn/anno)	27,341	32,811	37,353	41,057	46,266
Saved fuel (tonn/anno)	9373	11,248	12,805	14,074	15,860
Dumping (%)	0.0	0.0	5.3	11.3	22.7

Table 6
List of design characteristics for the determination of the capital cost of heat exchangers reported in Fig. 7.

Heat Exchanger	Type	Area (m^2)	N. of shell
E-101	Floating Head	844	3
E-102	Floating Head	68	1
E-103	Floating Head	322	1

We can conclude that scenario 3 is the most rewarding as it generate 0.41 M€/year of financial benefit in the economy of the plant. The aforementioned values of DFCROR are close to the upper limit of the range estimated by McKinsey using its Innomatics proprietary innovation database and tool that covers approximately 130 business units of leading chemical companies and gives rate of returns ranging between 5 and 10 % for new technological innovation in chemical processes in the

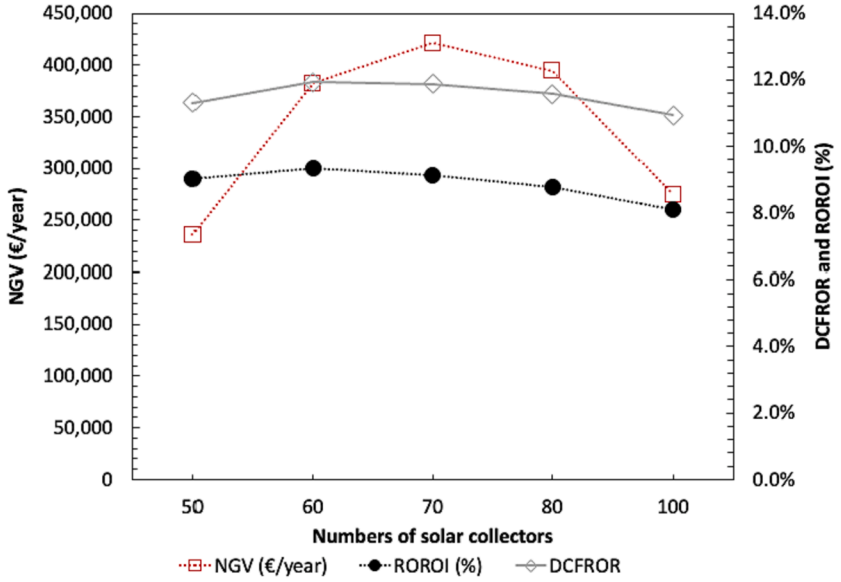

Fig. 10. Evaluation of the ROROI, and annual NGV of the integrated plant for the scenarios assumed in Table 5.

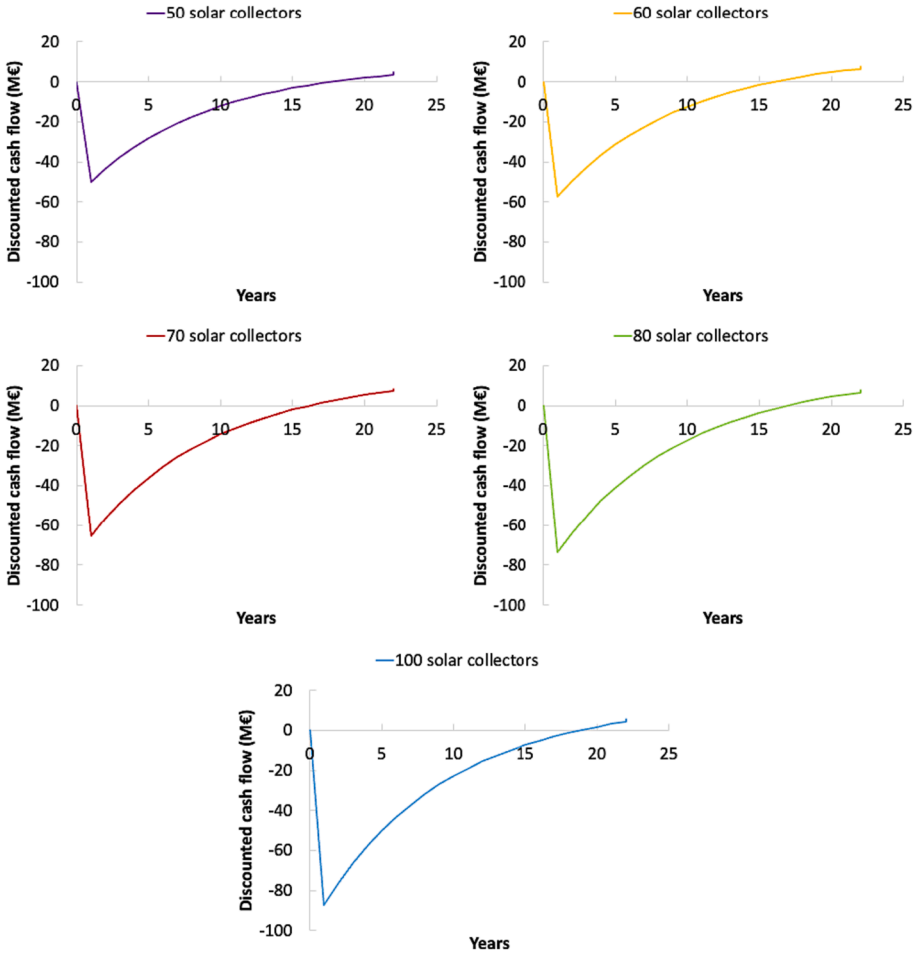

Fig. 11. Discounted Cash flow diagrams obtained downstream of the economic analysis performed for the dimensioned cases and shown in the Table 5.

market sector of commodity [45].

Conclusions

The chemical and petrochemical industries are among the largest energy consumers with an average annual growth of energy demand in the period 2000 – 2016 of 2 % associated with a 2.5 % yearly rate of increase in CO_2 emission. The achievement of suitable decarbonization strategy for this important sector would be an important goal to make more sustainable goods that are often difficult to be substituted.

In this context we wanted to study the possibility of using concentrated solar heat as renewable source in substitution of heat generated by combustion of methane to drive energy intensive endothermic processes.

The dehydrogenation of EB to STY was used as model process and the study was organized to find a chemical plant configuration compatible with the coupling with a CSP plant using a binary mixture $NaNO_3$/KNO_3, 60/40 w/w as HTF heated at 565 °C and to assess the economic sustainability of the hybridization strategy.

We found that a plant architecture based on a shell and tube fixed bed reactor can be adapted to the solar plant and can operate with 63 % conversion per pass of EB that makes possible a productivity of 103 kT/year of STY under isothermal regime provided that hot molten salt at 560–565 °C are fed to the shell with a flowrate of 200 kg/s. The residual enthalpy of the HTF exiting the reactor was further injected in the process by vaporizing and pre-heating ethylbenzene and water fed to the reactor.

Using a CSP plant of 70 collectors a reduction of emission of CO_2 of about 50 % can be obtained with a ROROI of 9.1 % and a DFCROR of 11.9 % for the solar part of the hybridized plant and with 410 k€/year of economic benefit for methane and CO_2 savings.

This study demonstrates that the use of concentrated solar heat can be an effective option to decarbonize energy intensive endothermic chemical processes.

CRediT authorship contribution statement

Claudia Prestigiacomo: Writing – original draft, Software, Methodology, Investigation, Conceptualization. **Federica Proietto:** Methodology, Investigation. **Alberto Giaconia:** Writing – original draft, Investigation, Conceptualization. **Monica Genovesi:** Software, Methodology, Investigation. **Najwa Hamdi:** Investigation. **Onofrio Scialdone:** Validation, Investigation, Formal analysis. **Alessandro Galia:** Writing – review & editing, Validation, Supervision, Funding acquisition, Conceptualization.

Declaration of competing interest

The authors declare that they have no known competing financial interests or personal relationships that could have appeared to influence the work reported in this paper.

Data availability

Data will be made available on request.

Acknowledgements

The results presented in this paper have been obtained in the framework of the “Concentrating Solar Power” project, under the “Electric System Research” program 2019–2021, with the financial support of Italian Ministry for Ecological Transition and in the framework of Project code PE0000021, Concession Decree No. 1561 of 11.10.2022 adopted by Ministero dell’Università e della Ricerca (MUR), CUP B73C22001280006 , Project title “Network 4 Energy Sustainable Transition – NEST”.

References

[1] Vooradi R, Babu Anne S, Tula AK, Eden MR, R.. Gani Vooradi, BMC. Chem Eng 2019;1:7.
[2] https://www.prnewswire.com/news-releases/global-styrene-market-outlook-on-size-trends-and-2020-key-player-analysis-report-301006589.html.
[3] Chemical and Engineering News. Facts and Figures for the Chemical Industry at a Glance 1989:36–45.
[4] Benjamin DH, Howard FR. In situ catalyst reactivation: used ethylbenzene dehydrogenation catalyst with agglomerated potassium promoter. Ind Eng Chem Prod Res Dev 1984;23:187–96.
[5] Howlett KE. The pyrolysis if 1,2–dichloroethane. Trans Faraday Soc 1952;25:25–34.
[6] James DH, Castor WM. Styrene. Ullmann’s Encyclopedia of Industrial Chemistry. A25. Wenham: Wiley-VCH; 1994. p. 329.
[7] Li C, Hu G, Zhong W, Du W, Qian F. Coke Deposition Influence Based on a Run Length Simulation of a 1,2–Dichloroethane Cracker. Ind Eng Chem Res 2013;52:17501–16.
[8] Hirsch D, Epstein M, Steinfeld A. The solar thermal decarbonization of natural gas. Int J Hydrogen Energy 2001;26:1023–33.
[9] Zedtwitz PV, Petrasch J, Trommer D, Steinfeld A. Hydrogen production via the solar thermal decarbonization of fossil fuels. Sol Energy 2006;80:1333–7.
[10] Hosseini SE, Wahid MA. Hydrogen from solar energy, a clean energy carrier from a sustainable source of energy. Int J Energy Res 2019;1:1–22.
[11] Chuayboon S, Abanades S. An overview of solar decarbonization processes, reacting oxide materials, and thermochemical reactors for hydrogen and syngas production. Int J Hydrogen Energy 2020;45:25783–810.
[12] Agrafiotis C, von Storch H, Roeb M, Sattler C. Solar thermal reforming of methane feedstocks for hydrogen and syngas production—a review. Renew Sustain Energy Rev 2014;29:656–82.
[13] De Falco M, Gallucci F. Ethanol steam reforming heated up by molten salt CSP: reactor assessment. Int J Hydr Eng 2010;35:3463–71.
[14] Manenti F, Leon-Garzon AR, Ravaghi-Ardebili Z, Pirola C. Assessing thermal energy storage technologies of concentrating solar plants for the direct coupling with chemical processes: the case of solar-driven biomass gasification. Energy 2014;75:45–52.
[15] Azadi P. An integrated approach for the production of hydrogen and methane by catalytic hydrothermal glycerol reforming coupled with parabolic trough solar thermal collectors. Int J Hydrogen Eng 2012;37:17691–700.
[16] Moretti C, Patil V, Falter C, Geissbühler L, Patt A, Steinfeld A. Technical, economic and environmental analysis of solar thermochemical production of drop-in fuels. Sci Total Environ 2023;901:166005.
[17] K. Lovegrove, W. Stein. Concentrating Solar Power Technology, Woodhead Publishing Limited 2012; ISBN 978-1-84569-769-3.
[18] Giaconia A, Iaquaniello G, Amin Metwally A, Caputo G, Balog I. Experimental demonstration and analysis of a CSP plant with molten salt heat transfer fluid in parabolic troughs. Sol Energy 2020;211:622–32.
[19] Wu C, Wang Q, Sun S, Wang X, Da Cui S, Pan HS. Comprehensive thermal properties of ternary eutectic molten salt/nanoparticles composite phase change materials for high–temperature thermal energy storage. Sol Energy Mater Sol Cells 2023;261:112531.
[20] Xie T, Zhang Z-Y, Zheng H-Y, Yu B, Q.. Xiao Performance optimization of a cavity type concentrated solar reactor for methane dry reforming reaction with coupled optics-CFD modeling. Chem Eng Sci 2023;275:118737.
[21] Martinek J, Bingham C, Weimer AW. Computational modeling of a multiple tube solar reactor with specularly reflective cavity walls. Part 2: Steam gasification of carbon. Chem Eng Sci 2012;81:285–97.
[22] Martinek J, Bingham C, Weimer AW. Computational modeling and on-sun model validation for a multiple tube solar reactor with specularly reflective cavity walls. Part 1: Heat transfer model. Chem Eng Sci 2012;81:298–310.
[23] Chambon M, Abanades S, Flamant G. Design of a lab-scale rotary cavity-type solar reactor for continuous thermal dissociation of volatile oxides under reduced pressure. Journal of Solar Energy Engineering, Transactions of the ASME 2010;132:0210061–7.
[24] Lichty P, Perkins C, Woodruff B, Bingham C, Weimer A. Rapid high temperature solar thermal biomass gasification in a prototype cavity reactor. Journal of Solar Energy Engineering, Transactions of the ASME 2010;132:0110121–7.
[25] Villafán-Vidales HI, Abanades S, Caliot C, Romero-Paredes H. Heat transfer simulation in a thermochemical solar reactor based on a volumetric porous receiver. Appl Therm Eng 2011;31:3377–86.
[26] Cisneros-Cárdenas NA, Pérez-Enciso RA, Pérez-Rábago CA, Calleja-Valdez RA, Maytorena-Soria VM, García-Gutiérrez R, et al. Cabanillas-Lopez Thermal experimental study of a volumetric receiver-reactor using a Mini-Solar furnace. Appl Therm Eng 2023;234:121276.
[27] Yeheskel J, Epstein M. Thermolysis of methane in a solar reactor for mass-production of hydrogen and carbon nano-materials. Carbon 2010;49:4695–703.
[28] Kochloefl K. Dehydrogenation of Ethylbenzene. In: Ertl G, Knozinger H, Weitkamp J, editors. Handbook of Heterogeneous Catalysis. 5. Weinheim: VCH; 1997. p. 2151.
[29] Giaconia A, Iaquaniello G, Caputo G, Morico B, Salladini A, Turchetti L, et al. Experimental validation of a pilot membrane reactor for hydrogen production by solar steam reforming of methane at maximum 550°C using molten salts as heat transfer fluid. Int J Hydrogen Energy 2020;45:33088–101.
[30] Giaconia A, Iaquaniello G, Morico B, Salladini A, Palo E. Techno-economic assessment of solar steam reforming of methane in a membrane reactor using molten salts as heat transfer fluid. Int J Hydrogen Energy 2021;46:35172–88.

[31] Giaconia A, Caputo G, Ienna A, Mazzei D, Schiavo B, O. Scialdone O, A. Galia,. Biorefinery process for hydrothermal liquefaction of microalgae powered by a concentrating solar plant: a conceptual study. Appl Energy 2017;208:1139–49.
[32] Giaconia A, Tizzoni AC, Sau S, Corsaro N, Mansi E, Spadoni A, et al. Assessment and perspectives of heat transfer fluids for csp applications. Energies 2021;14:7486.
[33] Stankiewicz A. Advances in modelling and design of multitubular fixed- bed reactors. Chem Eng Technol 1989;12:113–30.
[34] S. Carrà, L. Forni, Kinetics of catalytic dehydrogenation of ethylbenzene to styrene, l&EC process 44 design and development, 4 (1965).
[35] Benyahia F, O'Neill KE. Enhanced voidage correlations for packed beds of various particle shapes and sizes. Part Sci Technol 2005;23:169–77.
[36] Perry's chemical engineers' handbook. New York: McGraw-Hill.
[37] A. Miliozzi, G.M. Giannuzzi, P. Tarquini, A. La Barbera, ENEA Progetto solare ad alta temperatura: Fluido termovettore: dati di base della miscela di nitrati di sodio e potassio, ENEA/SOL/RD/2001/07, Rev. 0.0.
[38] C. Prestigiacomo, A. Giaconia, F. Proietto, G. Caputo, I. Balog, E. Ollà, C. Freni Terranova, O. Scialdone, A. Galia, Concentrated solar heat for the decarbonization of industrial chemical processes: a case study on crude oil distillation, submitted for publication, 2024.
[39] Giaconia A, Balog I, Caputo G. Hybridization of CSP plants: characterization of a molten salt heater for binary and ternary nitrate salt mixtures fueled with gas/biogas heaters. Energies 2021;14:7652.
[40] A.R. Darío Gómez, B. Watterson Branca, J.D. Americano, C. Ha, G. Marland, E. Matsika, L. Nenge Namayanga, B. Osman-Elasha, J.D. Kalenga Saka, K. Treanton, Chapter 2: Stationary Combustion 2006 IPCC Guidelines for National Greenhouse Gas Inventories, Energy 2.2 2 https://www.ipcc-nggip.iges.or.jp/public/2006gl/pdf/2_Volume2/V2_2_Ch2_Stationary_Combustion.pdf (2006).
[41] R. Turton, R.C. Bailie, W.B. Whiting, J.A. Shaeiwitz, Analysis, synthesis, and design of chemical processes, 3rd ed.
[42] International Renewable Energy Agency, The Power to Change: Solar and Wind Cost Reduction Potential to 2025 https://www.irena.org/-/media/Files/IRENA/Agency/Publication/2016/IRENA_Power_to_Change_2016.pdf (2016).
[43] G. Towler, R. Sinnot, Chemical Engineering Design: Principles, Practice and Economics of Plant and Process Design 2nd edition.
[44] Duncan A. Mellichamps, Internal rate of return: Good and bad features, and a new way of interpreting the historic measure. Comput Chem Eng 2017;106:396–406.
[45] M. Miremadi, C. Musso, J. Oxgaard, Chemical innovation: An investment for the ages, Copyright © 2013 McKinsey & Company. All rights reserved. Accessible at https://www.mckinsey.com/industries/chemicals/our-insights/chemical-innovation-an-investment-for-the-ages#/.